JOURNAL OF APPLIED ELECTROCHEMISTRY 20 (1990) 45–53

Nucleation and growth of anodic films on stainless steel alloys.

II. Kinetics of repassivation of freshly generated metal surfaces

F. J. GRAHAM, H. C. BROOKES*, J. W. BAYLES

Department of Chemistry, University of Natal, Durban 4001, South Africa

Received 31 August 1988; revised 9 May 1989

The kinetics of anodic film growth on six types of freshly generated stainless steel surfaces have been investigated electrochemically as a function of electrode potential and electrolyte composition. Repassivation of a scratch scar showed that initial growth of a passive film is controlled by ion migration in a high electric field obeying an inverse logarithmic rate law at passive potentials. The rate of growth was dependent on the electrode potential and the chloride ion concentration in the electrolyte. Three kinetically distinct regions were observed and are discussed in terms of film growth, film dissolution and pitting.

1. Introduction

The ability of a passive film to nucleate and to continue to grow, in order to passivate (or repassivate) a surface, is fundamental to the corrosion, especially pitting corrosion, behaviour of an alloy.

Many theoretical models have been proposed to explain the kinetics and mechanisms of film growth on metals. The most frequently reported rate laws for the growth of the passive film on iron and stainless steel alloys are the inverse logarithmic law and the direct logarithmic law. The former assumes that growth proceeds by ion conduction under high field conditions, while the latter assumes that a place exchange mechanism is responsible for the film growth. From chronoamperometric data, plots of logarithm of time against logarithm of current density provide a convenient diagnostic criterion for distinguishing between these rate laws.

Using a scratch chronoamperometric technique, Marshall and Burstein [1, 2] have shown that initial repassivation of a scratch scar on 316L (Cr 16.8; Ni 12.4; Mo 2.4; C 0.03; Fe bal. (wt %)) and 304L (Cr 18.3; Ni 10.6; C 0.03; Fe bal.) stainless steel electrode surfaces is controlled by ion conduction through the film under a high electric field. In alkaline media (1 M KOH), two kinetically distinct regions of film growth were found: the first occurring at short times, when the anodic charge passed is low; the second occurring at longer times. However, in acidic media, deviation from this relationship was observed [1, 2] some time into the transient. They ascribed this deviation of the current density to a 'constructive dissolution' process, that is, as the passivating film grows and the electric field strength across it relaxes, the iron component of the film begins to dissolve leaving the film enriched in chromium. The presence of Mo in the steel raises the electric field and so the dissolution occurs earlier in the repassivation process. Thus the onset of passivity is accelerated and hence the resistance to chloride-induced pitting is improved.

In this paper the kinetics of nucleation and growth of a passive film on stainless steel alloys [3] (Fe 18.5 Cr, 444, 4732, 4733, Fe18Cr3W and Fe17Cr6W) in 0.1 M H_2SO_4 and 0.1 M $HClO_4$ with varying Cl^- concentrations was investigated using a scratch chronoamperometric technique.

2. Experimental

The alloy composition, electrolytes, cell and instrumentation used in these scratch chronoamperometric experiments have been described previously [3]. All potentials are with respect to SSE.

The electrodes were polarized at a passive potential (−0.1 V) for 5 min before stepping to one of three potentials, namely, an active potential near the primary passivation potential, E_{pp}, a potential in the passive region and in the transpassive region (cf. Fig. 2 in [3]). The scratcher was then pulled rapidly across the width of both electrodes and the current transients for the repassivation of the scratch scars recorded on a dual channel digitizing oscilloscope (Nicolet 3091).

3. Results and discussion

The kinetics of the current density decay on scratched

* To whom correspondence should be addressed.

0021-891X/90 $03.00 + .12

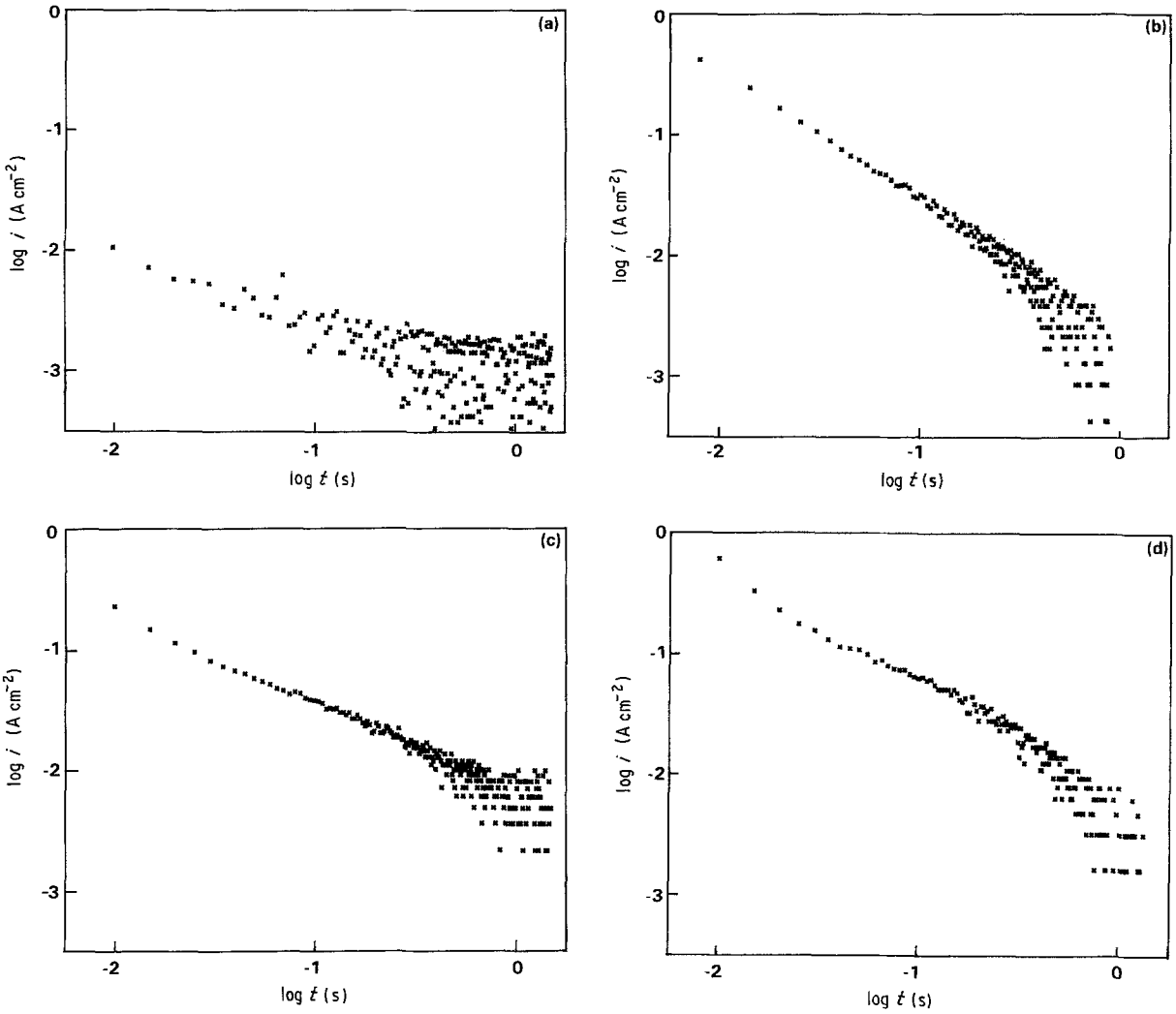

Fig. 1. Current transients on a scratched Fe18Cr3W alloy electrode in 0.1 M H_2SO_4 at (a) −870 mV (SSE), (b) −438 mV, (c) 0 mV, (d) 870 mV.

metal surfaces can be represented by log i as a function of log t and of q^{-1} in order to determine the rate law governing the repassivtion [1, 4–7].

3.1. *log* i *against log* t *analysis*

The logarithm of the anodic scratch current density decreased linearly with the logarithm of time yielding the empirical equation

$$\log i = -\alpha \log t + k \qquad (1)$$

where α is a constant, and it is proposed that k represents the current density of the bare metal surface before repassivation of the scratch scar. Figure 1

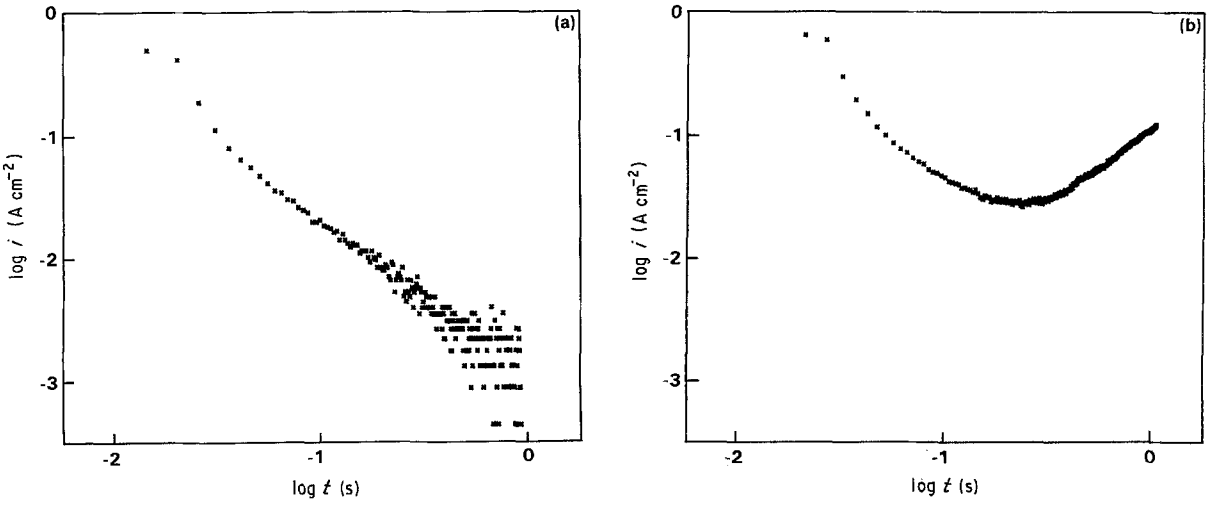

Fig. 2. Typical current transients on a scratched electrode (Fe18Cr is shown as an example) at 0 mV in (a) 0.1 M $HClO_4$ and (b) 0.1 M $HClO_4$ + 0.1033 M Cl^-.

Table 1. Values of α, the power in the general rate law for repassivation of the scratch scar, determined from log i against log t plots for certain alloys at various potentials and chloride ion concentrations in 0.1 M H_2SO_4 and in 0.1 M $HClO_4$†*

Alloy	E*(mV)*	*0 M* Cl^-		*0.01 M* Cl^-		*0.10 M* Cl^-	
		α	σ	α	σ	α	σ
444*	−870	−0.68	0.05	-	-	−0.65	0.02
	0	−1.22	0.04	−0.96	0.03	−0.94	0.02
	+870	−0.70	0.02	−0.75	0.03	−0.90	0.02
4732*	−870	−0.77	0.06	−0.78	0.06	−0.68	0.04
	0	-	-	−1.14	0.05	−0.96	0.04
	1000	−0.68	0.06	−0.91	0.04	−0.70	0.04
4733*	−870	−0.90	0.06	−0.74	0.05	−0.64	0.08
	0	−0.90	0.04	−0.96	0.04	−1.00	0.03
	+870	−0.84	0.04	−0.57	0.04	-	-
Fe18Cr3W*	−870	−0.70	0.07	−0.62	0.05	−0.58	0.03
	0	−0.99	0.02	−0.80	0.02	−0.80	0.02
	+870	−0.82	0.02	-	-	-	-
Fe17Cr6W*	−840	−0.86	0.05	−0.86	0.05	−0.86	0.05
	0	−0.90	0.05	−0.84	0.05	−0.86	0.02
	1000	−0.80	0.04	−0.70	0.04	-	-
Fe18.5Cr*	−870	−0.46	0.02	−0.48	0.01	−0.24	0.02
	0	−1.15	0.02	−1.11	0.02	−0.92	0.02
	+870	−0.91	0.04	−0.89	0.02	-	-
444†	−870	−0.79	0.09	−0.69	0.04	−0.68	0.03
	0	−1.03	0.03	−1.19	0.04	−0.37	0.01
	+870	−0.82	0.03	−0.83	0.02	−0.46	0.02
Fe18.5Cr†	−870	−1.27	0.07	−0.85	0.03	−0.57	0.02
	0	−0.65	0.01	−1.00	0.01	−0.37	0.01
	+870	−0.84	0.05	−0.75	0.04	−0.22	0.03

σ is the standard deviation found.

shows typical plots of log i as a function of log t for the repassivation of stainless steels in 0.1 M H_2SO_4. The gradients of these plots, given in Table 1, yield the power, α, of the general rate law for repassivation of the scratch scars. Linearity according to Equation 1 is achieved over 1.5 to 2 decades of current density and time. Deviations from linearity at longer times will be discussed below. In the presence of Cl^- a change in the gradients of these plots was usually observed, the extent of which was dependent on the alloy and potential as can be seen in Table 1.

Replacement of 0.1 M H_2SO_4 with 0.1 M $HClO_4$ results in plots of log i against log t that are qualitatively the same as those shown in Fig. 1, although loss of linearity occurs at lower Cl^- concentrations (0.01 M) and at lower potentials for a given Cl^- concentration. At high Cl^- concentrations (0.1 M), an inflection point is observed in the log i against log t plot (Fig. 2), which was not observed in the pure 0.1 M H_2SO_4 electrolyte. This point occurs at lower $[Cl^-]$ for the less corrosion resistant alloys. Extensive general and pitting corrosion was evident on subsequent SEM examination of the electrode surface, which also was not seen with the H_2SO_4 electrolyte. Thus, it is suggested that the inflection point arises because the rate of active dissolution of the passive film and alloy is greater than that of repassivation and film growth. It is evident that the nature of the anions in the bulk electrolyte influences the repassivation and subsequent stability of the passive film, with SO_4^{2-} having a greater stabilizing effect than ClO_4^- in the presence of Cl^-. These results support previous findings [8] in which the influence of anions on the pitting behaviour of stainless steels was investigated.

For a given electrolyte composition, the greatest scatter of data points and deviation from linearity was observed when the electrodes were scratched while held at active potentials (Fig. 1). At −870 mV ($\approx E_{pp}$) non-linearity is due to the passive film having just started to form, for alloys 444, 4732 and 4733, and as such cannot effectively passivate the entire scratched surface for any appreciable length of time (≈3s), while for alloys Fe18.5Cr, Fe18Cr3W and Fe17Cr6W a protective passive film would not yet have started to form because −870 mV is ≈20 mV cathodic to E_{pp} for these alloys. At passive potentials (Fig. 1c), greater linearity is observed, with the gradient of the line becoming steeper and the scatter of data points being reduced, as can be seen from the standard deviation values in Table 1. At transpassive potentials departure from linearity at both short and long times is observed and a decrease in the gradient of the line occurs.

Deviations from linearity at small t (≤20 ms) can be due to several factors amongst which the following deserve consideration:

1. Scratching is not instantaneous, with repassivation of the scratch scar commencing prior to completion of the generation of the scratch. $t = 0$ is assigned to that value of t midway between t (commencement of the scratch, that is, the initial rise in the current density) and t (completion of scratch generation, that is, the maximum current density preceeding the current decay). Thus the error in the position of $t = 0$ when calculating, for example, the charge density subsequent to scratching the electrode, is only large when short periods of time (< 15 ms) after scratching are considered, as opposed to the error when calculating the charge density 200 ms after scratching.

2. The initial high current density is due to the dissolution of the alloy, prior to coverage of the bare surface by a film, which marks the onset of the linear region.

The current response was monitored for two seconds after scratching, to determine whether the current density either continued to decay, or had reached a limiting value or began to increase. Thus deviations from linearity at large values of t (≥250 ms) occur as a result of either growth and thickening of the passive film, or of irreparable breakdown of the passive film and subsequent alloy dissolution. In the latter case the current density increases as a function of time (Fig. 2b), while in the former, a 'block' of data points is observed beneath the straight line as shown, for example, in Fig. 1b, c. These results were verified by subsequent SEM examination of the electrode surfaces. While small pits were observed on the surfaces for cases where the current density increased, there was no evidence of pitting for transients exhibiting the 'block' of data points.

Despite the scatter of experimental data points, and

with the exception of alloy Fe17Cr6W, certain general trends were observed in both 0.1 M H_2SO_4 and 0.1 M $HClO_4$, namely: (i) an increase in α as the Cl^- concentration was increased: (ii) the α values obtained at active and near active potentials (−870 to −840 mV) and in solutions of high Cl^- concentrations (0.1 M) are greater than those at passive potentials, 0 mV, and at lower [Cl^-] (0.01 M). The latter values show that the initial film growth, on repassivation of the scratch scar, follows the inverse logrithmic rate law [4]. The evidence suggests that at potentials and Cl^- concentrations at which the passive film is not stable a different rate law or a combination of rate laws, if the transition is not well defined, pertains. This change in the rate law with the onset of passivation is not unlikely since it has been shown previously [9–12] that the greatest influence of the minor alloying elements is observed at active, active–passive transition and transpassive potentials where, it has been suggested, they alter the passive film composition [13–15] and the rate of film growth.

3.2. *log* i *against* q^{-1} *analysis*

After repassivation of the scratch scar, continued growth of the passive film requires the migration of ionic species and this only occurs at a measurable rate in the presence of large electric fields (10^6 V cm^{-1}). The current flowing when ions are conducted through an oxide film may be represented by [5–7, 16]

$$i = 2A \sinh (BV/x) \quad (2)$$

where V is the potential drop across a film of thickness x and A and B are parameters related to the energy barrier through which the mobile ions pass.

Equation 2 may be simplified to

$$i = A \exp (BV/x) \quad (3)$$

in the presence of a large electric field across the film. Burstein and Marshall [1, 6] have shown that the initial anodic charge, q, flowing from a newly generated metal surface, goes exclusively into film formation, and no significant metal dissolution occurs. The

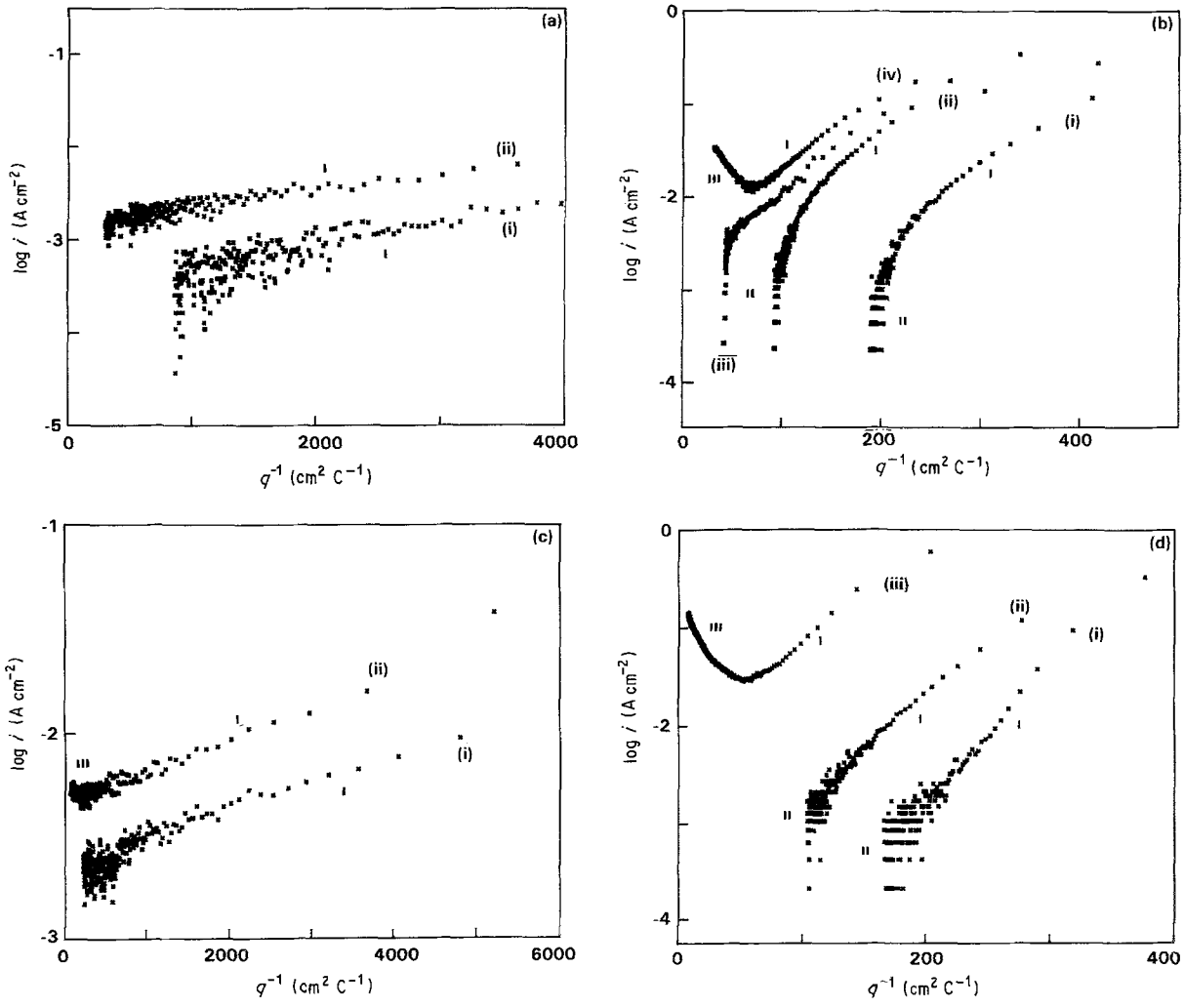

Fig. 3. Repassivation of a scratched 444 alloy electrode at: (a) −870 mV in (i) 0.1 M H_2SO_4, (ii) 0.1 M H_2SO_4 + 0.1 M Cl^-; (b) 0 mV in (i) 0.1 M H_2SO_4, (ii) 0.1 M H_2SO_4 + 0.1 M Cl^-; 870 mV in (iii) 0.1 M H_2SO_4, (iv) 0.1 M H_2SO_4 + 0.1 M Cl^-. Fe18.5Cr alloy electrode at: (c) −870 mV in (i) 0.1 M H_2SO_4, (ii) 0.1 M H_2SO_4 + 0.1 M Cl^-; (d) 0 mV in (i) 0.1 M H_2SO_4, (ii) 0.1 M H_2SO_4 + 0.01 M Cl^-; (iii) 0.1 M H_2SO_4 + 0.1 M Cl^-. 4733 alloy electrode at: (e) −870 mV in (i) 0.1 M H_2SO_4, (ii) 0.1 M H_2SO_4 + 0.1 M Cl^-; (f) 0 mV in (i) 0.1 M H_2SO_4, (ii) 0.1 M H_2SO_4 + 0.1 M Cl^-; 870 mV in (iii) 0.1 M H_2SO_4, (iv) 0.1 M H_2SO_4 + 0.1 M Cl^-. Fe17Cr6W alloy electrode at: (g) −870 mV in (i) 0.1 M H_2SO_4, (ii) 0.1 M H_2SO_4 + 0.1 M Cl^-; (h) 0 mV in (i) 0.1 M H_2SO_4, (ii) 0.1 M H_2SO_4 + 0.1 M Cl^-; (j) 870 mV in (i) 0.1 M H_2SO_4, (ii) 0.1 M H_2SO_4 + 0.1 M Cl^-.

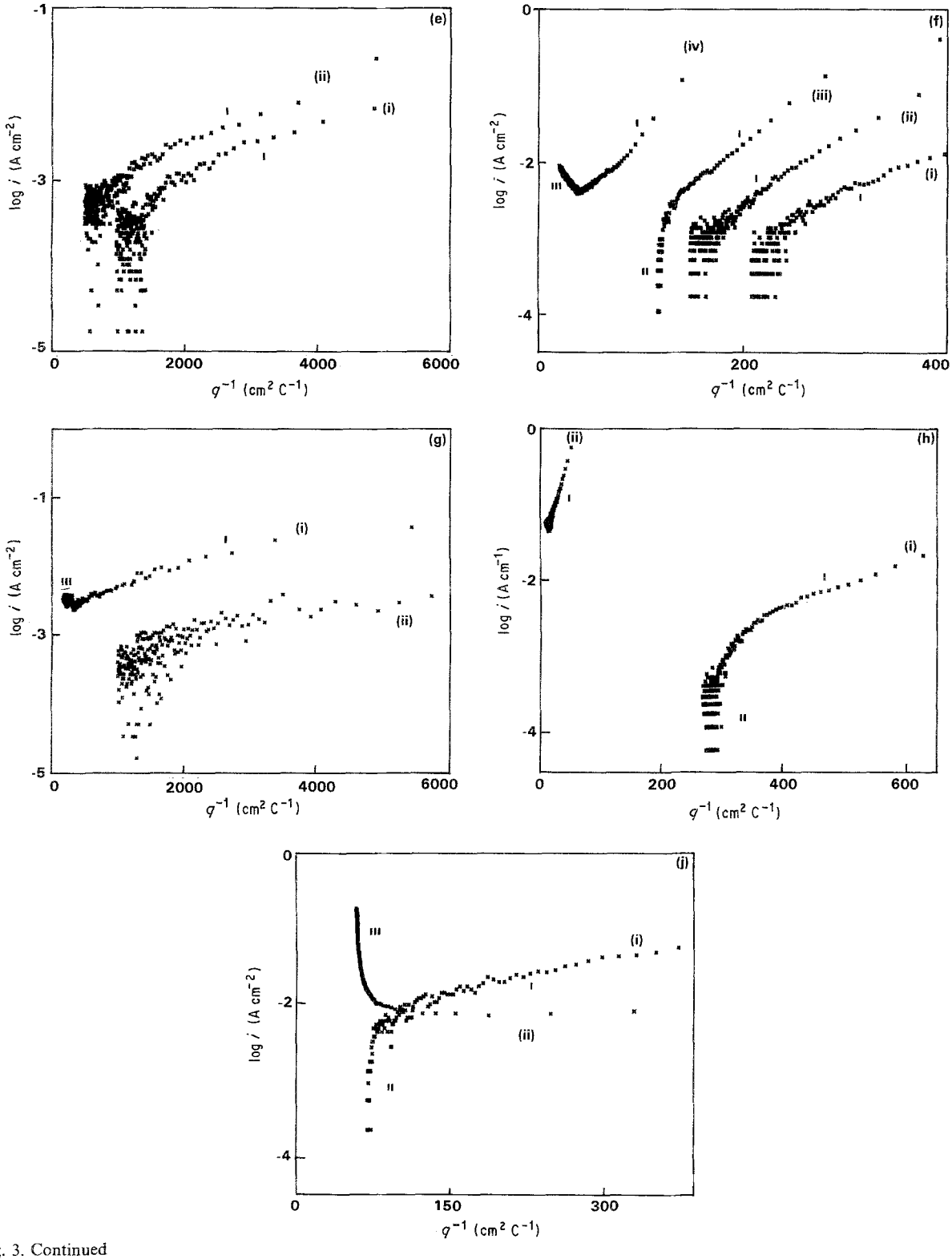

Fig. 3. Continued

film thickness can therefore be related to the charge per unit area, q, which has flowed from the scratch from $t = 0$ to t

$$q = \frac{zF\varrho x}{M} \tag{4}$$

where ϱ is the density of a film of molecular mass M, z is the number of electrons by which each metal atom has been oxidized and F is Faraday's constant. Substituting Equation 4 into Equation 3, gives

$$\log i = \log A + \frac{BVzF\varrho}{2.3\,Mq} \tag{5}$$

In accordance with Equation 5 the data were subsequently examined by plotting log i as a function of q^{-1}.

3.2.1. 0.1 M H_2SO_4. Figure 3 illustrates typical kinetic plots for alloys Fe18.5Cr, 444, 4733 and Fe17Cr6W in 0.1 M H_2SO_4 as a function of applied potential and Cl^- concentration. In 0.1 M H_2SO_4, the more corrosion resistant alloys (444, 4733 and to a lesser extent 4732 — to be referred to hereafter as 'the 444 group') yield a linear plot when stepped to $\approx E_{pp}$ (−870 mV) before scratching (Fig. 3a). An explanation for the

scatter of data points and deviation from linearity at short and long times is similar to that given above. For the less corrosion resistant alloys (the Fe18.5Cr group, namely Fe18.5Cr, Fe18Cr3W and Fe17Cr6W) an inflection point, the significance of which will be discussed later, is present at high values of q (Fig. 3c). This inflection point (from regions I to II) becomes more prominent in Cl^- containing solutions and at transpassive potentials and suggests that the poor stability and protective ability of the passive film, under the given experimental conditions, results in alloy dissolution.

Scratching the electrodes, when polarized at a passive potential, results in a sharp increase in the gradient of the initial part of the log i against q^{-1} curve (compare Figs. 3a,c with Figs. 3b,d, respectively). Equation 5 predicts a linear relationship between log i and q^{-1}. At passive and transpassive potentials (the latter in the absence of high Cl^- concentrations) two linear regions of the high field decay laws are encountered as repassivation of the scratch scar proceeds. As shown in Fig. 3b,d,f, the first region (I) occurs at high current densities, at the commencement of the current decay, indicating initial repassivation of the scratch scar, and the second region (II) at intermediate values, namely, the commencement of a steady state current density, which suggests effective repassivation of the scratch scar.

Increasing the Cl^- concentration reduces the scatter of data points. This is particularly noticeable with the less corrosion resistant alloys (Fig. 3d,g). On addition of 0.1 M Cl^- the second region (II) is replaced by a third region (III) (Fig. 3b,d,f,j). For a given potential this phenomenon occurs at lower Cl^- concentrations for the Fe18.5Cr group alloys than for the 444 group alloys (that is, in the presence of 0.01 M Cl^- as opposed to 0.1 M Cl^-); and for a given electrolyte composition, region (III) occurs at more cathodic potentials for the Fe18.5Cr group alloys than for the 444 group (that is at 0 mV as opposed to 870 mV). The presence of region (III) indicates that the rate of dissolution is exceeding the rate of repassivation and growth.

3.2.2. 0.1 M $HClO_4$. Replacing 0.1 M H_2SO_4 with 0.1 M $HClO_4$ resulted in the same trends as those described above, namely; for a given potential, as the Cl^- concentration is increased, the slope of region (I) increases and the scatter of data points decreases; and for a given Cl^- concentration, as the potential is made more anodic, region (II) is replaced by region (III). The slopes of these plots were greater for 0.1 M $HClO_4$ than for 0.1 M H_2SO_4, particularly subsequent to the addition of 0.1 M Cl^-.

The changes in shape of the log i against q^{-1} plots are summarized schematically in Fig. 4. These plots give an indication as to the nature of the passive film at specific potentials and electrolyte compositions. The first linear section (I) of these curves concerns the inital repassivation of the scratch surface and could correspond to the formation of a surface film (thickness $\approx$ 1 to 2 monolayers, as discussed below) at active potentials, and to film thickening at passive and transpassive potentials. If the potential of the electrode and the Cl^- concentration are such that growth of the passive film is possible, a second linear region (II) develops. It is suggested that the hatched region corresponds to the breakdown and repair of the oxide film. The width of the hatched area is determined by the stability of the passive film and the length of time that the transient is recorded, while the height is a function of the net breakdown and repair current flowing – repair determining the lower and breakdown determining the upper limits of the region. Considering the −870 mV data, for example Fig. 3e, with 0.1 M H_2SO_4 as the electrolyte, this 'block' of data points commences after approximately 500 $\mu C\,cm^{-2}$ have flowed, which is the typical charge density expected for the formation of one monolayer of divalent oxide. At higher Cl^- concentrations (0.1 M) this value increases to approximately 1000 $\mu C\,cm^{-2}$

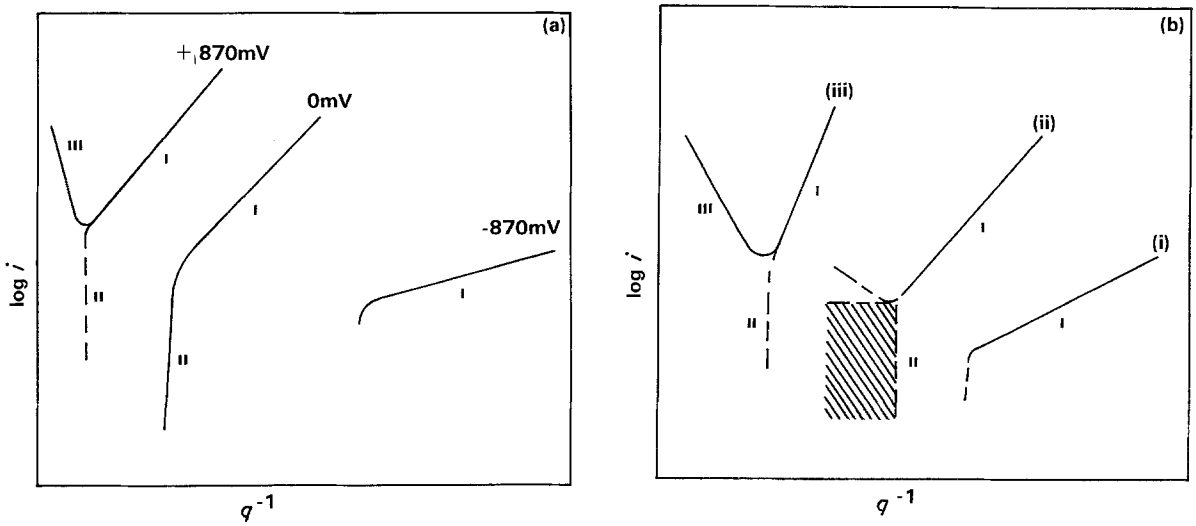

Fig. 4. Schematic representation of the effect on the log i against q^{-1} plot for a stainless steel alloy in 0.1 M H_2SO_4, subsequent to scratching the electrode surface, of varying (a) the applied potential, for a given electrolyte composition, and (b) the chloride ion concentration of the electrolyte for a given applied potential: (i) 0.1 M H_2SO_4; (ii) 0.1 M H_2SO_4 + 0.01 M Cl^-; (iii) 0.1 M H_2SO_4 + 0.1 M Cl^-. Hatched region: see text.

suggesting that not all the current density recorded is due to film formation and growth, but that a certain fraction is due to alloy dissolution or that two layers are formed before breakdown and repair of the surface film commences. Region (III) appears at potentials and Cl^- concentrations that do not support passive film growth. The presence and continued increase of region (III) indicates the initiation and propagation of pitting corrosion, as was verified by subsequent SEM examination of the electrode surface. It is possible that a critical Cl^- concentration and film thickness (related to q) exists for the transition from region (II) to region (III). When a film grows and the film thickness increases, the electric field strength across the passive film will decrease resulting in the subsequent dissolution of the passive film, or part thereof, with a corresponding net current increase. It is this passive film breakdown and dissolution that is responsible for the appearance of region (III). As the weakening of the electric field strength across the entire electrode surface is unlikely to be uniform, localized corrosion will result.

3.2.3. Kinetic parameters A *and* B *from plots of* $d\log i/dq^{-1}$ *against* E. For regions (I) and (II), assuming that the potential across the film is constant and independent of the film thickness, the potential may be given by [6]

$$V = E - E_g \tag{6}$$

where E is the electrode potential and E_g is the minimum electrode potential required to cause film growth by high field ion conduction. E_g can thus be calculated since

$$\frac{\mathrm{d}\log i}{\mathrm{d}\, q^{-1}} = \frac{BzF\varrho}{2.3M}(E - E_g) \tag{7}$$

A linear relationship between d log i/d q^{-1} and E, validating Equation 7, was obtained (Fig. 5) and allowed E_g to be determined for each alloy. From the E_g values given in Table 2 it can be seen that as the Cl^- concentration increases E_g becomes more anodic or remains constant for all alloys except 4732 and

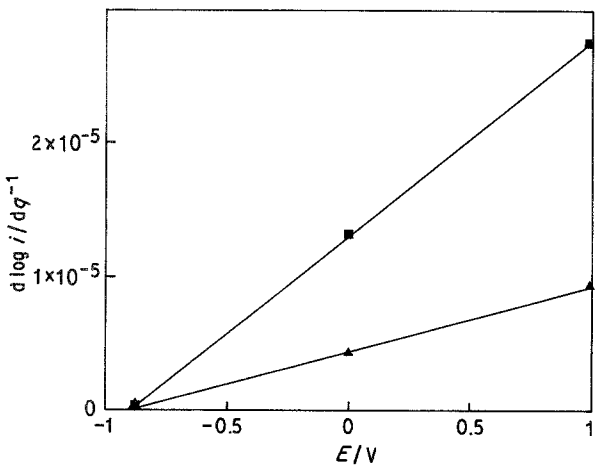

Fig. 5. Plots of d log i/d q^{-1} against E, for region (I), for alloy 4732 in 0.1 M H_2SO_4 + 0.01 M Cl^- (■) and in 0.1 M H_2SO_4 + 0.1 M Cl^- (▲), for the determination of E_g.

Table 2. E_g values for various stainless steel alloys

Alloy	E_g *(mV w.r.t. SSE)*		
	0 M Cl^-	*0.01 M* Cl^-	*0.1 M* Cl^-
Fe18.5Cr*	−889	−887	−887
444*	−893	−893	−892
Fe18Cr3W*	−898	−930	−929
4732*	−910	−905	−926
Fe17Cr6W*	−930	−929	−926
4733*	−931	−914	−902
Fe18.5Cr†	−935	−930	−926
444†	−940	−902	−889

* In 0.1 M H_2SO_4.
† In 0.1 M $HClO_4$.

Fe18Cr3W. It should, however, be noted that the error in the E_g values could be as large as ±15 mV depending on alloy composition and applied potential. An anodic shift is understandable because, as the Cl^- concentration increases and the alloys become less corrosion resistant, a larger active potential region would be expected, resulting in a shift in E_g to more anodic potentials. These results are supported by anodic polarization experiments [17] in which E_{Flade} either shifted to more anodic potentials as the Cl^- concentration increased, or remained constant while the current density at E_{Flade} increased — hence the passive current density attained in 0.1 M H_2SO_4 will only be reached at more anodic potentials. The E_g values obtained in 0.1 M $HClO_4$ are more cathodic than in H_2SO_4, thus supporting previous findings [3, 17] which showed that although the passive film formed as rapidly in $HClO_4$ as in H_2SO_4, the film formed in the latter had a greater long term stability, and was more resistant to Cl^- attack, than a film formed in $HClO_4$.

Having determined E_g, the second kinetic parameter, B, associated with film growth could be calculated using Equation 5, with $\varrho = 5.7\,\mathrm{g\,cm^{-3}}$, $M = 70\,\mathrm{g\,mol^{-1}}$ and $z = 2$; these values being suitable for an iron–chromium oxyhydroxide film [6].

For a given alloy the values of B for region (I), although almost independent of potential, increased by $\sim 2.5 \times 10^{-7}\,\mathrm{cm\,V^{-1}}$ on increasing the Cl^- concentration from 0 to 0.1 M Cl^-; for example alloy 444 at −870 mV: $0.86 \times 10^{-6}\,\mathrm{cm\,V^{-1}}$ (0.1 M H_2SO_4), $1.08 \times 10^{-6}\,\mathrm{cm\,V^{-1}}$ (0.1 M H_2SO_4 + 0.1 M Cl^-); and at 0 mV: $1.20 \times 10^{-6}\,\mathrm{cm\,V^{-1}}$ (0.1 M H_2SO_4), $1.46 \times 10^{-6}\,\mathrm{cm\,V^{-1}}$ (0.1 M H_2SO_4 + 0.1 M Cl^-). The B values obtained for alloys Fe18.5Cr, 4733 and 444 (average $1.3 \times 10^{-6}\,\mathrm{cm\,V^{-1}}$) are in general agreement with those obtained by Burstein and co-workers [1, 2, 6, 18] for 304L and 316L stainless steel in acidic and alkaline media. Our values for 4732, Fe18Cr3W and Fe17Cr6W are typically about half the above magnitude (average $6 \times 10^{-7}\,\mathrm{cm\,V^{-1}}$). The values of B obtained for region (II), where present, were at least an order of magnitude greater than those of region (I). These results are not unexpected as the parameters, A and B, are a direct function of the energy barrier

through which mobile ions must pass to achieve film growth and thus variations in the growth rate, and possibly film composition and structure, due to alloy composition and experimental conditions would be expected to be reflected by varying values of A and B.

The values of A show a greater degree of scatter with no systematic change with respect to potential, Cl^- concentration or alloy composition. These were also the findings of Burstein and co-workers [1, 2, 6, 18]. Such variations in A are feasible in that the mobile ions will experience different activation energies, depending on the stage of film growth, experimental conditions and the nature of the interface.

3.3. *Influence of minor alloying elements*

A possible explanation for the results presented in this paper is that molybdenum, tungsten and, to a lesser extent, vanadium are passive in the active potential region of iron and chromium. Thus after scratching the electrode surface of, for example, a FeCrMo alloy, a molybdenum enriched oxide film may form, owing to the slower dissolution rate of molybdenum, which in turn reduces the rate of dissolution of the alloy. From the Pourbaix diagram for the Mo–H_2O system [19] it can be seen that at low potentials it is the inhibiting effect of elemental molybdenum that reduces the active dissolution. Hashimoto [20] suggests the subsequent formation of a passive, hydrated chromium or iron oxyhydroxide film which grows beneath this molybdenum enriched film. Once the scratch has been repassivated the molybdenum enriched film dissolves leaving the newly formed passive chromium/iron oxyhydroxide film to protect the alloy. At more anodic potentials, in the passive region, the effect is not as dramatic owing to the transpassive dissolution of molybdenum. This proposal is supported by ESCA analysis [9–11] in which a molybdenum enriched passive film (both Mo(IV) and elemental Mo were detected) was found at potentials in the vicinity of E_{pp} but not at more anodic potentials. From the respective Pourbaix diagrams it is apparent that tungsten, and to a lesser extent vanadium, could act in a similar manner. However, very little data has been published on the compositional profiles of the passive films formed on tungsten- and vanadium-containing alloys. From the data presented in this paper it is seen that the response of the vanadium alloys, as shown by alloy 4733 in Fig. 3, is very similar to that of the molybdenum containing alloy 444. This supports previous results from anodic polarization (i.e. pitting behaviour) [8, 17], cyclic voltammetric [17] and conventional chronoamperometric (rising transients) [21] experiments. Tungsten additions to a Fe18Cr alloy, as found previously [8, 17], do not improve the passive film's stability or resistance to Cl^- attack. As shown in Fig. 3g,h,j the addition of 0.1 M Cl^- to 0.1 M H_2SO_4 results in a dramatic change in the shape of the log i against q^{-1} curves with region (III) being evident at all potentials in the range -1.0 to $+1.0$ V. Thus, considering the influence of minor alloying elements, it may be concluded that whereas molybdenum (1.8 wt %) and vanadium (2.7 and 4.1 wt %) additions to a Fe18Cr alloy have a beneficial effect on the stability of the passive film and its resistance to attack by chloride ions in acidic media, tungsten additions (3.0 and 5.7 wt %) have a detrimental effect, especially in the presence of chloride ions.

4. Conclusions

1. The rate of initial film growth on a freshly generated scratch scar is controlled by high field ion conduction.

2. Two successive high field mechanisms occur, which may be followed by dissolution of the surface film, owing to a decrease in the electric field strength.

3. The above three processes are dependent on the alloy composition, $[Cl^-]$ and applied potential.

4. At passive potentials initial film growth, in 0.1 M H_2SO_4 and 0.1 M $HClO_4$ with $[Cl^-] \leqslant 0.01$ M follows the inverse logarithmic rate law.

5. At potentials and Cl^- concentrations at which the passive film is not stable, a combination of rate laws is observed.

6. Addition of 1.8 wt % Mo, 2.7 wt % V and 4.1 wt % V to a Fe18Cr alloy have a beneficial effect on the stability of the surface film and its resistance to attack by chloride ions in acidic media, whereas addition of 3.0 wt % W and 5.7 wt % W have a detrimental effect, especially in the presence of chloride ions.

Acknowledgements

We thank the Foundation for Research Development (CSIR) and the University Research Fund for financial support, and ISCOR for alloys.

References

[1] P. I. Marshall and G. T. Burstein, *Corros. Sci.* **24** (1984) 463.
[2] G. T. Burstein and P. I. Marshall, *Corros. Sci.* **24** (1984) 449.
[3] H. C. Brookes, J. W. Bayles and F. J. Graham, *J. Appl. Electrochem.* in press.
[4] H. -J. Rätzer-Scheibe, in 'Passivity of Metals and Semiconductors' (edited by M. Froment), Elsevier, Amsterdam (1983) p. 731.
[5] M. J. Dignam, in 'Comprehensive Treatise of Electrochemistry', Vol. 4 (edited by J. O'M. Bockris, B. E. Conway, E. Yeager, R. E. White) Plenum, New York (1981) chapter 5.
[6] G. T. Burstein and P. I. Marshall, *Corros. Sci.* **23** (1983) 125.
[7] J. W. Schultz, M. M. Lohrengel and D. Ross, *Electrochim. Acta.* **28** (1983) 973.
[8] H. C. Brookes and F. J. Graham, *Corrosion* in press.
[9] I. Olefjord and B. -O. Elfstrom, *Corrosion* **38** (1982) 46.
[10] I. Olefjord and B. Brox, in 'Passivity of Metals and Semiconductors' (edited by M. Froment) Elsevier, Amsterdam (1983) p. 561.
[11] I. Olefjord and B. -O. Elfstrom, *Corros. Sci.* **15** (1975) 697.
[12] R. C. Newman and E. M. Franz, *J. Electrochem. Soc.* **131** (1984) 223.
[13] K. Doss, A. Brooks and C. Clayton, *Int. Cong. Met. Corr.* **1** (1984) 138.
[14] M. Frolicher, A. Hugot-Le Goff and V. Jovancicevic, in 'Passivity of Metals and Semiconductors' (edited by M. Froment) Elsevier, Amsterdam (1983) p. 85.

[15] T. Ohtsuka, K. Azumi and N. Sato, *ibid.*, p. 199.
[16] T. P. Hoar, in 'Modern Aspects of Electrochemistry', No. 2, (edited by J. O'M. Bockris) Butterworths, London (1959) p. 262.
[17] F. J. Graham, MSc Thesis, Univ. Natal (1987).
[18] G. T. Burstein and G. W. Ashley, *Corrosion* **40** (1984) 110.
[19] M. Pourbaix, 'Atlas of Electrochemical Equilibria in Aqueous Solutions', Pergamon, London (1966) p. 187.
[20] K. Hashimoto, in 'Passivity of Metals and Semiconductors' (edited by M. Froment) Elsevier, Amsterdam (1983) p. 247.
[21] H. C. Brookes and F. J. Graham, to be published.